PHYSICAL REVIEW E **69**, 016602 (2004)

Large phase shift of nonlocal optical spatial solitons

Qi Guo,[1,2,*] Boren Luo,[1] Fahuai Yi,[3] Sien Chi,[1] and Yiqun Xie[2]
[1]*Institute of Electro-Optical Engineering, National Chiao Tung University, Hsinchu, Taiwan, China*
[2]*Laboratory of Light Transmission Optics, South China Normal University, Guangzhou, Guangdong, China*
[3]*Department of Mathematics, South China Normal University, Guangzhou, Guangdong, China*
(Received 26 June 2003; revised manuscript received 7 October 2003; published 14 January 2004)

In this paper, we discuss the evolution of the optical beam in nonlocal cubic nonlinear media, modeled by the nonlocal nonlinear Schrödinger equation (NNLSE). A different approximate model to the NNLSE is presented for the strongly nonlocal media with arbitrary response functions. An exact analytical solution of the model is obtained, and a spatial soliton is found to exist. A different phenomenon is revealed that the phase shift of such a nonlocal optical spatial soliton can be very large comparable to its local counterpart. The stability of the solution is rigorously proved. The comparisons of our analytical solution with the numerical simulation of the NNLSE, as well as with Snyder-Mitchell (linear) model [A. W. Snyder and D. J. Mitchell, Science **276**, 1538 (1997)] are given.

DOI: 10.1103/PhysRevE.69.016602 PACS number(s): 42.65.Tg, 42.65.Jx, 42.70.Df, 42.70.Nq

I. INTRODUCTION

Interest in properties of an optical spatial soliton in nonlocal nonlinear media, called a nonlocal optical spatial soliton in this paper, has greatly grown during recent years both theoretically [1–8] and experimentally [9]. The nonlocal optical spatial soliton is modeled by the nonlocal nonlinear Schrödinger equation (NNLSE) [1,4,6] that the nonlinear term assumes a nonlocal form (convolution integral) with a symmetric and real-valued response kernel, while the NNLSE also describes several other physical situations [7,8]. According to the degree of the nonlocality determined by the relative width of the response kernel and the optical beam (or the other wave packets for more general cases), there are four categories of the nonlocality [6,8]: local, weakly nonlocal, generally nonlocal, and strongly nonlocal. Snyder and Mitchell [1] simplified the NNLSE to a linear model in the strongly nonlocal case, and found an exact Gaussian-shaped stationary solution to the model called as an accessible soliton. Their work was highly appreciated by Shen [10]. So far, more properties of solitons modeled by NNLSE and the related phenomena have theoretically been opened out. A study by a variational approach was carried out with respect to the specific power-law response kernel [3], and a tractable model of the logarithmic nonlocal nonlinear media with the Gaussian response kernel was presented [4]. Subwavelength nonlocal spatial solitons were also studied [5]. Exact soliton solutions in the limit of weak nonlocality [7] were obtained, modulational instabilities were analyzed [6], and the properties of soliton stabilization with arbitrary degree of nonlocality [8] were investigated. Following these achievements, we present here a model to simply the NNLSE in the strongly nonlocal case, and an exact analytical solution to the model is found, which reveals a phenomenon that the phase shift of the strongly nonlocal optical spatial soliton, the spatial soliton in the strongly nonlocal media, can be very large.

Structurally, the paper develops the thesis in the following way. In Sec. II, we present an approximate model to the NNLSE with arbitrary response function by means of the Taylor's expansion of the response function, and obtain an exact analytical solution to the model. We also show the equivalence of the evolution equation for the beam width to Newton's second law for the motion of a particle in classic mechanics. Section III is concerned with the discussion of the solution. The analytical solution is compared with the numerical propagation of the NNLSE, and a phenomenon of a large phase shift of the strongly nonlocal optical spatial soliton is explored. The result about a rigorous proof for the stability of the solution is given in Sec. IV. In Sec. V a comparison is made of our model with Snyder-Mitchell (linear) model. Section VI is conclusion.

II. SIMPLIFIED MODEL OF THE NNLSE AND ITS ANALYTICAL SOLUTION

The propagation of the optical beam in the nonlocal cubic nonlinear media is modeled by the NNLSE [1,4,6]

$$i\frac{\partial\psi}{\partial z}+\mu\triangle_{\perp}\psi+\rho\psi\int R(\mathbf{x}-\mathbf{x}')|\psi(\mathbf{x}',z)|^2d^D\mathbf{x}'=0, \quad (1)$$

where $\psi(\mathbf{x},z)$ is a paraxial beam, $\mu=1/2k$, $\rho=k\eta$, k is the wave number in the media without nonlinearity (that is, $k=\omega n_0/c$, and n_0 is the linear refractive index of the media), η is a material constant ($\eta>0$ or <0 corresponds to a focusing or defocusing material), z is the longitudinal (propagation direction) coordinate, $\mathbf{x}$ and $\mathbf{x}'$ are the D-dimensional transverse coordinate vectors ($\mathbf{x},\mathbf{x}'\in\mathbb{R}^D$, $D=1$ or 2), $d^D\mathbf{x}'$ is a D-dimensional volume element at $\mathbf{x}'$, $\triangle_{\perp}$ is the D-dimensional transverse Laplacian operator, and the integration limits are $-\infty$ and ∞. Here, R is normalized symmetrical real spatial response of the media such that $\int R(\mathbf{x}')d^D\mathbf{x}'=1$.

For the strongly nonlocal case, we have $w/w_m<1$, where w and w_m are the beam width and the width of the response

*Electronic address: guoq@scnu.edu.cn

function, i.e., the characteristic length of the material, then the response function $R(\mathbf{x})$ can be expanded in Taylor's series. Concretely, we first expand the response $R(\mathbf{x}-\mathbf{x}')$ with respect to $\mathbf{x}'$ about $\mathbf{x}'=0$ (the beam center in the primed coordinate system) to the second order in the first integral over $\mathbf{x}'$, then expand again the functions $R^{(j)}(\mathbf{x})$ in the result of the first integrand, where $R^{(j)}(\mathbf{x})$ denotes $\partial^j R(\mathbf{x})/\partial x_1^{j-i}\partial x_2^i$ (x_1 and x_2 are the transverse coordinates, $j=0,1,2$, $i=0,j$), with respect to $\mathbf{x}$ about $\mathbf{x}=0$ till all of the $R^{(2)}(0)$ terms appear before evaluation of the second integral over $\mathbf{x}$. In this way, the NNLSE can be deduced as [11]

$$i\frac{\partial\psi}{\partial z}+\mu\nabla_\perp^2\psi+\rho\psi\int\left[R_0+\frac{1}{2}R_0''(\mathbf{x}-\mathbf{x}')^2\right]|\psi(\mathbf{x}',z)|^2 d^D\mathbf{x}' =0, \tag{2}$$

where $R_0=R(\mathbf{x}')|_{\mathbf{x}'=0}$, and $R_0''=\partial_{x_1}^2 R(\mathbf{x}')|_{\mathbf{x}'=0}$, which turns out to be for z-axial symmetrical solution $\psi(r,z)$:

$$i\frac{\partial\psi}{\partial z}+\frac{\mu}{r^{D-1}}\frac{\partial}{\partial r}\left(r^{D-1}\frac{\partial}{\partial r}\psi\right)-\frac{1}{2}\rho\gamma P_0 r^2\psi+\rho R_0 P_0\psi -\frac{1}{2}\rho\gamma\psi\int|\psi(r',z)|^2 r'^2 d^D\mathbf{x}'=0, \tag{3}$$

where $r=|\mathbf{x}|$ is the transverse distance from the beam center in the coordinate system without the prime, $\gamma=-R_0''>0$ [$R_0''<0$ because R_0 is a maximum of $R(\mathbf{x})$], $P=\int|\psi(\mathbf{x},z)|^2 d^D\mathbf{x}$ is the beam power [12], and P_0 is the input power at $z=0$. The substitution of P_0 for P in the third and fourth terms above follows the fact that power P is conserved [13]. Equation (3) is our model for solutions.

We search for a solution to Eq. (3) of the Gaussian function form

$$\psi(r,z)=\frac{\sqrt{P_0}\exp[i\theta(z)]}{[\sqrt{\pi}w(z)]^{D/2}}\exp\left[-\frac{r^2}{2w(z)^2}+ic(z)r^2\right], \tag{4}$$

where θ is the phase of the complex amplitude of the solution, w is beam width, c represents the phase-front curvature of the beam, and they are all allowed to vary with propagation distance z. The real amplitude of the solution has the form $\sqrt{P_0}/[\sqrt{\pi}w]^{D/2}$, owing to the conservation of the power. Inserting the trial function above into Eq. (3), and from the coefficient of the zero-order term of r, we obtain a first-order ordinary differential equation for θ

$$\frac{d\theta}{dz}+\frac{D\mu}{w^2}-\frac{1}{4}\rho P_0(4R_0-D\gamma w^2)=0. \tag{5a}$$

In the same way, the real and imaginary parts of the coefficient of r's quadratic term yield the two equations for the parameters w and c, respectively,

$$\frac{dw}{dz}-4\mu c w=0, \tag{5b}$$

$$\frac{dc}{dz}-\frac{\mu}{w^4}+4\mu c^2+\frac{1}{2}\rho\gamma P_0=0. \tag{5c}$$

The combination of Eq. (5c) with the derivative form of Eq. (5b) yields

$$\frac{1}{\mu}\frac{d^2y}{dz^2}-\frac{4\mu}{w_0^4y^3}+2\rho\gamma P_0 y=0, \tag{6}$$

where the normalization that $w(z)/w_0=y(z)$ is introduced, and $w_0=w(0)$.

Equation (6) is equivalent to Newton's second law in classical mechanics for the motion of an one-dimensional particle with the equivalent mass $1/\mu$ acted by the equivalent force $F=4\mu/w_0^4y^3-2\rho\gamma P_0 y$, while y and z are equivalent to the spatial and temporal coordinates of the particle, respectively. The first term of F makes the particle accelerated, and has the particle's velocity dy/dz becoming bigger and bigger, which means that the beam is being expanded or has a trend to be expanded, depending upon the initial velocity $dy/dz|_{z=0}\geqslant 0$ or <0. It is obvious that this term is the effect of diffraction. By contrast, the second term of F, which acts as an elastic force following Hooke's law that always drives the particle back to its initial state if $\rho>0$ (i.e., $\eta>0$), decelerates the particle, and presents the compression effect of nonlinearly induced refraction. When the diffractive force and the refractive force have the same amplitude, the total force will be zero, and the particle will keep its velocity unchangeable. Then the particle with initial zero velocity keeps rest, and its spatial coordinate y is always 1: this is a spatial soliton state. Letting the two forces equal and $y=1$, we obtain the critical (input) power for the soliton propagation

$$P_c=\frac{2\mu}{\gamma\rho w_0^4}=\frac{1}{\gamma w_0^4 k^2\eta}. \tag{7}$$

It is observed that F is a conservative force, because F can be expressed as $F(y)=-dV(y)/dy$, and the equivalent potential $V(y)$ is given by

$$V(y)=\frac{2\kappa(y^2-1)(y^2-\Lambda)}{\mu w_0^2 y^2}, \tag{8}$$

where $\kappa=\mu\rho\gamma P_0 w_0^2/2=w_0^2\eta\gamma P_0/4$, and $\Lambda=P_c/P_0$. Therefore, the total energy of the equivalent particle that equals $E=T+V$ is a constant of the motion, where $T=(dy/dz)^2/2\mu$ is its kinetic energy (It is reminded here that $1/\mu$ is the mass of the particle.). Assuming that the beam at $z=0$ has $dw(z)/dz|_{z=0}=0$ [14] such that the particle's initial total energy is zero, then $T+V=0$ gives the following equation

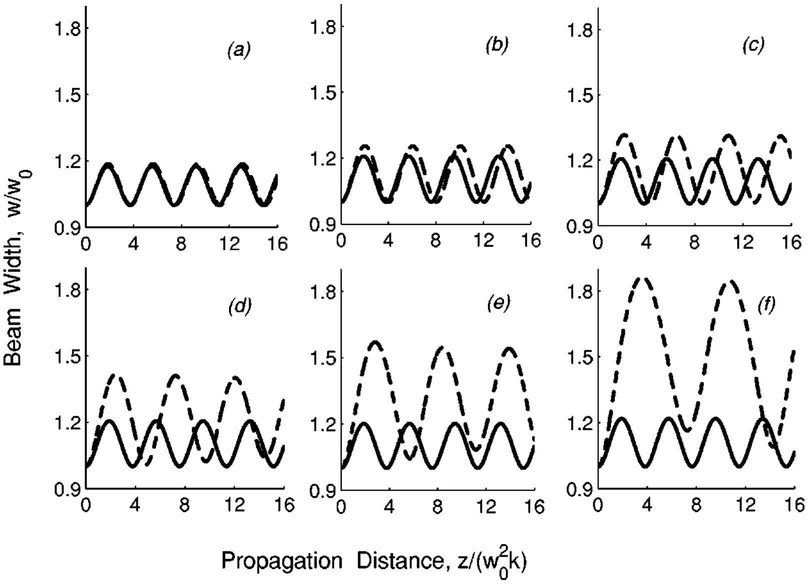

FIG. 1. Comparison of analytical solution (solid curves) with numerical simulation (dashed curves) for the (1+1)-dimensional beam propagation in the Gaussian-shaped response material when $P_0<P_c$. The initial conditions are (a) $w_0/w_m=0.1$, (b) $w_0/w_m=0.2$, (c) $w_0/w_m=0.3$, (d) $w_0/w_m=0.4$, (e) $w_0/w_m=0.5$, (f) $w_0/w_m=0.6$, and $P_0/P_c\approx0.7$ for all cases.

$$\frac{1}{2}\left(\frac{dy}{dz}\right)^2+\frac{2\kappa(y^2-1)(y^2-\Lambda)}{w_0^2y^2}=0. \tag{9}$$

As a matter of fact, direct one-time integration of Eq. (6) also yields Eq. (9) mathematically.

For the materials with positive η, we have $\kappa>0$ and $\Lambda>0$. Then integration of Eq. (9) reads

$$w^2=w_0^2\left[\cos^2(\beta_0z)+\frac{P_c}{P_0}\sin^2(\beta_0z)\right], \tag{10}$$

where $\beta_0=2\sqrt{\kappa}/w_0=(\gamma\eta P_0)^{1/2}$. The substitution of Eq. (10) into Eq. (5a) and Eq. (5b) yields, respectively,

$$\theta=-\frac{D}{2}\arctan\left[\sqrt{\frac{P_c}{P_0}}\tan(\beta_0z)\right]+\frac{D(1-P_0/P_c)}{16kw_0^2\beta_0}\sin(2\beta_0z)+\rho R_0P_0z-\frac{D(P_0/P_c+1)z}{8kw_0^2}, \tag{11}$$

and

$$c=\frac{\beta_0k(P_c/P_0-1)\sin(2\beta_0z)}{4[\cos^2(\beta_0z)+(P_c/P_0)\sin^2(\beta_0z)]}. \tag{12}$$

Then by the substitution of Eqs. (10)–(12) into Eq. (4), we obtain the exact solution of Eq. (3):

$$\psi(r,z)=\frac{\sqrt{P_0}}{(\sqrt{\pi}w)^{D/2}}\exp\left(-\frac{r^2}{2w^2}\right)\exp[i(cr^2+\theta)], \tag{13}$$

which satisfies the initial condition at $z=0$

$$\psi(r,0)=\frac{\sqrt{P_0}}{(\sqrt{\pi}w_0)^{D/2}}\exp\left(-\frac{r^2}{2w_0^2}\right), \tag{14}$$

where w, θ, and c are given by Eqs. (10), (11), and (12).

III. DISCUSSION ABOUT THE SOLUTION: LARGE PHASE SHIFT

The Gaussian-shaped solution derived here is the exact solution to Eq. (3), but the approximate one to Eq. (1) for the strongly nonlocal case. Equation (10) shows that when $P_0<P_c$, beam diffraction initially overcomes beam-induced refraction, and the beam initially expands, with w^2/w_0^2 vibrating between a maximum P_c/P_0 and a minimum 1; whereas when $P_0>P_c$, the reverse happens and the beam initially contracts, with w^2/w_0^2 breathing between a maximum 1 and a minimum P_c/P_0. When $P_0=P_c$, diffraction is exactly balanced by nonlinearity, and the Gaussian-shaped beam preserves its width as it travels in the straight path along z axis. This is a soliton. These features of the $(1+D)$-dimensional beam ($D=1$ or 2) are shown in Figs. 1–6, where the analytical solutions are compared with the results of numerical propagation of Eqs. (1) and (14) for different w_0/w_m and P_0. To simulate the propagation, we assume the material response is the Gaussian function [4,6]

$$R(r)=\frac{1}{(\sqrt{2\pi}w_m)^D}\exp\left(-\frac{r^2}{2w_m^2}\right). \tag{15}$$

Tables I and II give the exact numerical results, the analytical results, and their relative errors for the maximums (or minimums) of the on-axis normalized amplitude $|\psi(0,z)|/\psi(0,0)$ for the parameters given in these six corresponding figures. Clearly the (1+1)-dimensional analytical predictions are in agreement with the exact numerical simulations when $w_0/w_m\leqslant0.1$, and still close approximation (the absolute values of the relative errors are within 10%) to the simulations till w_0/w_m reaches 0.4 for the $P_0<P_c$ case, and 0.5 for the

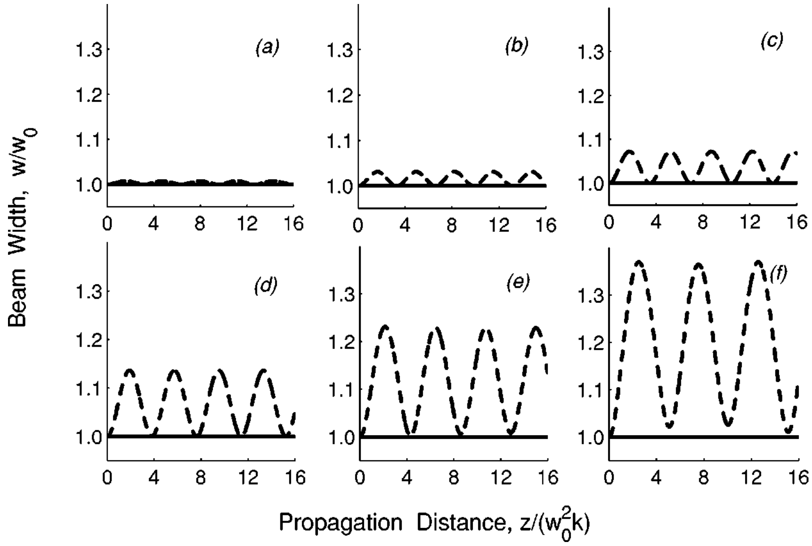

FIG. 2. Comparison of analytical solution (solid curves) with numerical simulation (dashed curves) for the (1+1)-dimensional beam propagation in the Gaussian-shaped response material when $P_0 = P_c$. The initial conditions are (a) $w_0/w_m = 0.1$, (b) $w_0/w_m = 0.2$, (c) $w_0/w_m = 0.3$, (d) $w_0/w_m = 0.4$, (e) $w_0/w_m = 0.5$, and (f) $w_0/w_m = 0.6$.

$P_0 = P_c$ and $P_0 > P_c$ cases. For the same w_0/w_m, the higher the input power, the better the approximation. The approximations of the (1+2)-dimensional analytical results to the corresponding numerical ones are a little bit worse than the (1+1)-dimensional cases.

When $P_0 = P_c$, Eq. (13) is simplified to a soliton expression

$$\psi_s(r,z) = \frac{\exp(i\phi z)}{\pi^{D/4} w_0^{2+D/2} (\gamma\eta)^{1/2} k} \exp\left(-\frac{r^2}{2w_0^2}\right), \quad (16)$$

where $\phi = 3D(4\sigma/3D - 1)/(4w_0^2 k)$, $\sigma = R_0/\gamma w_0^2$, and ϕz is the phase shift after propagating a distance z. The spatial soliton of this kind existing in the strongly nonlocal media is called the strongly nonlocal optical spatial soliton. A strongly nonlocal optical spatial soliton with any width can propagate in the media as long as its power P_0 equals exactly the critical power P_c defined in Eq. (7). It should be paid attention that σ is a parameter determined by the initial beam width and the material property. To illuminate this, we use the relation $\gamma = -R_0'' \sim R_0/w_m^2$, then $\sigma = \nu w_m^2/w_0^2$, where the proportional coefficient ν is determined only by the material property, and $|\nu|$ has an order of 1. For example, if the response of the material is assumed to be the Gaussian function (15), it can be shown that $\nu = 1$ independent of D. For the strong nonlocality, we have $w_m/w > 1$. Supposing we take $w_m/w_0 \geqslant 5$, then it is observed that $\phi z \approx \nu w_m^2 z/w_0^4 k$. For local Kerr soliton, it has been shown that the phase shift $\phi_l z = z/(2kw_0^2)$ for (1+1)-dimensional case [15]. Comparing the results between the strongly nonlocal and the local cases, we observe that the phase shift for the former is $(w_m/w_0)^2$ times (about two order) larger than that for the latter provided $w_m/w_0 \geqslant 10$. Figures 7 and 8 are the comparison of the phase evolutions from our model and the numerical simulation, and Table III gives the relative error between the numerical and analytical results of the on-axis phase slope. Obviously our phase solution is in very close agreement with the numerical simulation when w_0/w_m is much smaller than 1; while our result is still closely approximate to the numerical simulation when w_0/w_m becomes gradually bigger, ap-

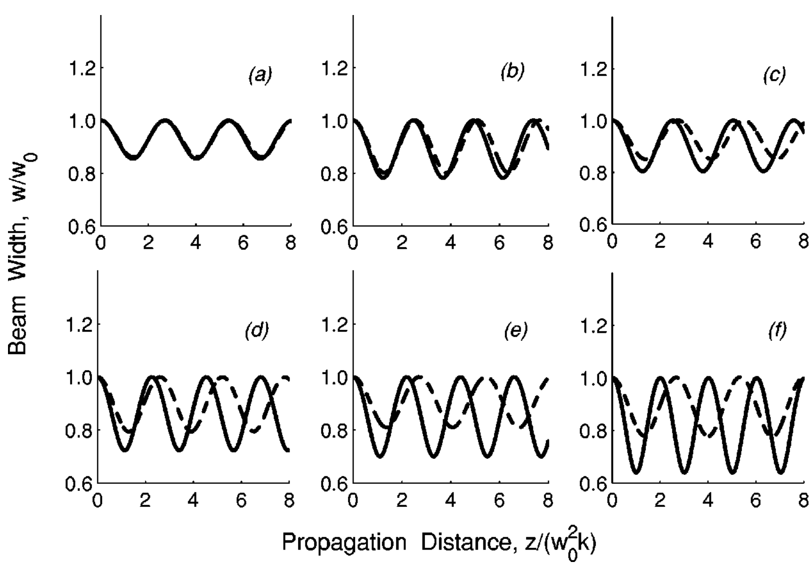

FIG. 3. Comparison of analytical solution (solid curves) with numerical simulation (dashed curves) for the (1+1)-dimensional beam propagation in the Gaussian-shaped response material when $P_0 > P_c$. The initial conditions are (a) $w_0/w_m = 0.1$, $P_0/P_c = 1.37$, (b) $w_0/w_m = 0.2$, $P_0/P_c = 1.63$, (c) $w_0/w_m = 0.3$, $P_0/P_c = 1.55$, (d) $w_0/w_m = 0.4$, $P_0/P_c = 1.91$, (e) $w_0/w_m = 0.5$, $P_0/P_c = 2.04$, and (f) $w_0/w_m = 0.6$, $P_0/P_c = 2.44$.

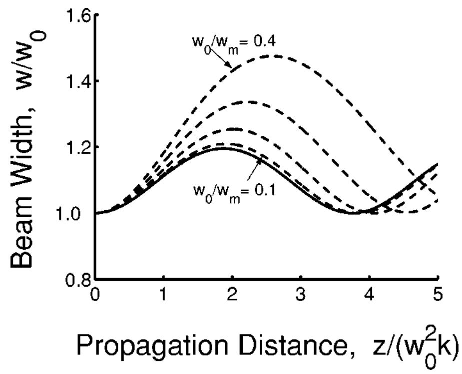

FIG. 4. Comparison of analytical solution (solid curves) with numerical simulation (dashed curves) for the (1+2)-dimensional beam propagation in the Gaussian-shaped response material when $P_0/P_c=0.7$. For the numerical result, the parameter w_0/w_m is 0.1, 0.2, 0.3, and 0.4, respectively from down to up.

proaching but being less than 1, no matter that $D=1$ or 2. We, therefore, conclude that the phase shift of the Gaussian-shaped spatial soliton can be very large during it propagates in strongly nonlocal media comparable to its local counterpart.

In the same way, the phase shift for nonsoliton case can be obtained by analyzing Eq. (11).

The physical origin of the phenomenon can qualitatively be understood from the term "nonlocality." Nonlinear nonlocality means that the nonlinear polarization of media with a small volume of radius r_0 ($r_0 \ll$ any wavelength involved) depends not only on the value of the electric field inside this volume (at the present time and in the past), but also on the electric field outside the volume under consideration. The stronger the nonlocality, the more fields are involved to contribute to the polarization, hence the larger phase shift is obtained.

The effective generation of a large phase shift is very important for the modification, manipulation, and control of optical fields based on the principle of interference, especially in the optical switching [16], hence the finding about the large phase shift of the strongly nonlocal optical spatial solitons might be found to be of potential value in applications.

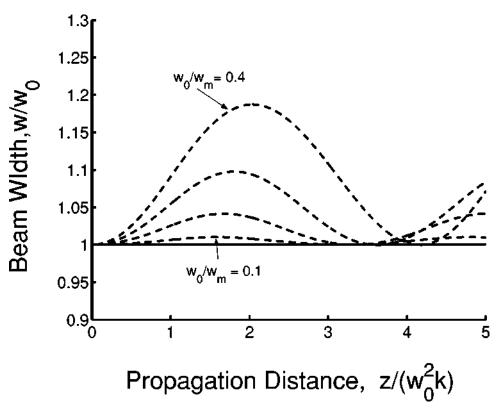

FIG. 5. Comparison of analytical solution (solid curves) with numerical simulation (dashed curves) for the (1+2)-dimensional beam propagation in the Gaussian-shaped response material when $P_0/P_c=1$. For the numerical result, the parameter w_0/w_m is 0.1, 0.2, 0.3, and 0.4, respectively, from down to up.

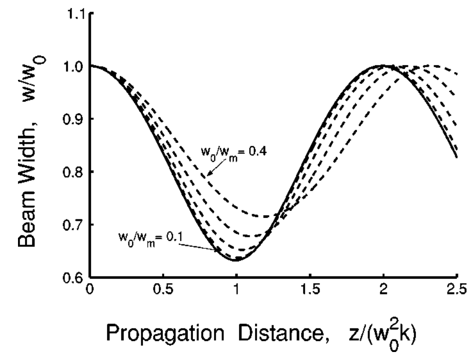

FIG. 6. Comparison of analytical solution (solid curves) with numerical simulation (dashed curves) for the (1+2)-dimensional beam propagation in the Gaussian-shaped response material when $P_0/P_c=2.5$. For the numerical result, the parameter w_0/w_m is 0.1, 0.2, 0.3, and 0.4, respectively, from down to up.

IV. PROOF OF THE STABILITY OF OUR MODEL

An important content of the solution search for nonlinear equations is the stability analysis of their solutions. The stability property of the particular solution (13) to Eq. (3) for the initial condition (14) has been obtained. The mathematical prerequisites for this stability demonstration are only calculus, specially Schwarz inequality, as well as the other three inequalities in elementary mathematics [17], and no more advanced mathematical knowledge is needed. Only the conclusion is given here; details about the formal proof will be given elsewhere.

TABLE I. The exact numerical results, the analytical results, and their relative errors for the maximums (or minimums) of the on-axis normalized amplitude $|\psi(0,z)|/\psi(0,0)$ in the (1+1)-dimensional case.

w_0/w_m	0.1	0.2	0.3	0.4	0.5	0.6
For the parameters in Fig. 1 ($\lvert\psi(0,z)\rvert$ has the minimum)						
ER[a]	0.919	0.894	0.869	0.837	0.799	0.750
AR[b]	0.922	0.910	0.911	0.911	0.912	0.906
RE(%)[c]	−0.3	−1.8	−4.8	−8.8	−14.1	−20.8
For the parameters in Fig. 2						
ER	0.996	0.985	0.967	0.941	0.910	0.864
AR	1.000	1.000	1.000	1.000	1.000	1.000
RE(%)	−0.4	−1.5	−3.4	−6.3	−9.9	−15.7
For the parameters in Fig. 3 ($\lvert\psi(0,z)\rvert$ has the maximum)						
ER	1.078	1.116	1.082	1.118	1.111	1.134
AR	1.082	1.131	1.115	1.176	1.195	1.250
RE(%)	−0.4	−1.3	−3.0	−5.2	−7.6	−10.2

[a]ER: exact numerical results to Eqs. (1) and (14).
[b]AR: analytical approximate results to Eq.(1), $|\psi(0,z)|_{\max}[|\psi(0,z)|_{\min}]/\psi(0,0)=(P_0/P_c)^{1/4}$.
[c]RE: relative errors, RE=(ER−AR)/ER.

TABLE II. The exact numerical results, the analytical results, and their relative errors for the maximums (or minimums) of the on-axis normalized amplitude $|\psi(0,z)|/\psi(0,0)$ in the (1+2)-dimensional case.

w_0/w_m	0.1	0.2	0.3	0.4
For the parameters in Fig. 4 ($\lvert\psi(0,z)\rvert$ has the minimum)				
ER	0.846	0.791	0.747	0.655
AR[a]	0.851	0.827	0.829	0.830
RE(%)	−1.1	−4.3	−10.9	−26.7
For the parameters in Fig. 5				
ER	0.990	0.960	0.913	0.846
AR	1.000	1.000	1.000	1.000
RE(%)	−1.0	−4.0	−9.5	−18.1
For the parameters in Fig. 6 ($\lvert\psi(0,z)\rvert$ has the maximum)				
ER	1.159	1.234	1.147	1.208
AR	1.170	1.279	1.244	1.383
RE(%)	−0.9	−3.6	−8.3	−14.4

[a] $|\psi(0,z)|_{\max}[|\psi(0,z)|_{\min}]/\psi(0,0)=(P_0/P_c)^{1/2}$.

Assume that $\Psi(\mathbf{x},z)$ is the solution of the following Cauchy problem:

$$i\frac{\partial\Psi}{\partial z}+\mu\nabla_\perp^2\Psi+\rho\Psi\int\left[R_0-\frac{\gamma}{2}(\mathbf{x}-\mathbf{x}')^2\right]|\Psi(\mathbf{x}',z)|^2d^D\mathbf{x}'=0,\quad \mathbf{x},\mathbf{x}'\in\mathbb{R}^D,\quad z>0 \tag{17a}$$

$$\Psi(\mathbf{x},0)=\Psi_0=\psi_0+f(\mathbf{x}),\quad \mathbf{x}\in\mathbb{R}^D, \tag{17b}$$

where $f(\mathbf{x})$ is the random perturbation and $\psi_0=\psi(r,0)$ given by Eq. (14).

Let $u(\mathbf{x},z)=\Psi(\mathbf{x},z)-\psi(r,z)$. We have rigorously demonstrated that $u(\mathbf{x},z)$ satisfies the inequality

$$\int(|u|^2+|u|^2r^2+|\nabla_\perp u|^2)d^D\mathbf{x}\leqslant\Pi\int(|f|^2+|f|^2r^2+|\nabla_\perp f|^2)d^D\mathbf{x}, \tag{18}$$

where Π is a finite constant. Then we have the fact that as long as $f\to0$, u will be trend 0, i.e., $\Psi(\mathbf{x},z)\to\psi(r,z)$.

V. COMPARISON OF OUR MODEL WITH SNYDER-MITCHELL MODEL

In the case where the characteristic length of the material w_m is much larger than the beam width w, in the other words, that mathematically w_m trends to infinite or relatively w trends to zero, $|\psi(r',z)|^2$ within the integration of Eq. (3) can be considered to be δ function of the variable r' such that the last term of Eq. (3) equals zero. If the last second term of Eq. (3) is considered to be zero, it can be dropped. Therefore, for the conditions under consideration, without taking its last two terms, i.e., zero-order terms of r, into account, Eq. (3) can be simplified to the linear model suggested by Snyder and Mitchell [1]

$$i\frac{\partial\psi}{\partial z}+\frac{\mu}{r^{D-1}}\frac{\partial}{\partial r}\left(r^{D-1}\frac{\partial}{\partial r}\psi\right)-\frac{1}{2}\rho\gamma P_0r^2\psi=0. \tag{19}$$

As mentioned in the foregoing, the evolution of the beam width and the phase-front curvature is determined by the quadratic term of r, while the phase's evolution comes from the zero-order term of r. Hence it is obvious that the results about w and c from our model are the same with that from Snyder-Mitchell model. Because they emphasized on the evolution of the beam width, however, Snyder and Mitchell did not discuss the phase evolution in Ref. [1].

Except the difference in form, there is another difference between two models in methodology. Our model is obtained by direct expansion of R within the integration, but R is first taken out from the integration and then expanded to yield Snyder-Mitchell model. As has been mentioned, this requires mathematically w_m tends to infinite or equivalently w tends to zero. As a result, degree of nonlocality in our model is

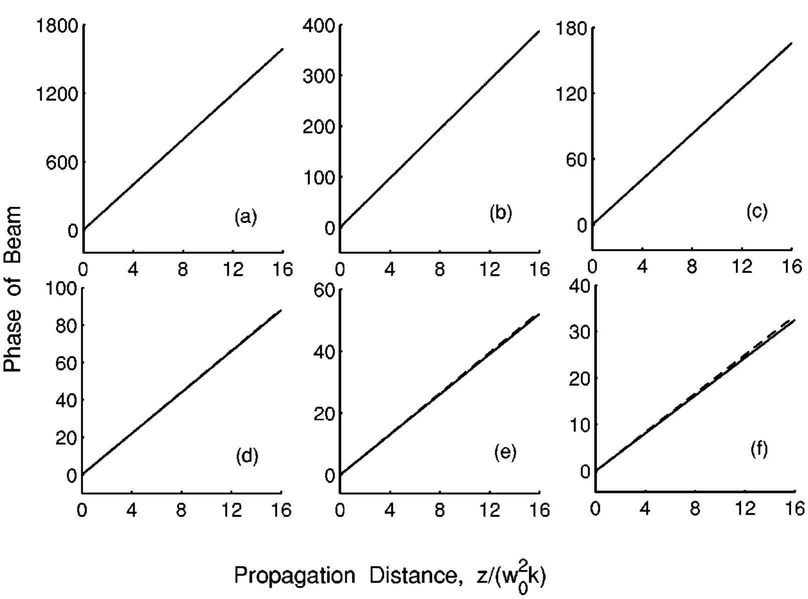

FIG. 7. Comparison of the results about the phase from our model (solid curves) and the numerical simulation (dashed curves) for the (1+1)-dimensional beam propagation in the Gaussian-shaped response material when $P_0=P_c$. Another initial condition is (a) $w_0/w_m=0.1$, (b) $w_0/w_m=0.2$, (c) $w_0/w_m=0.3$, (d) $w_0/w_m=0.4$, (e) $w_0/w_m=0.5$, and (f) $w_0/w_m=0.6$. For simulation results, there are included three phase curves corresponding to the on-axis and two-side at $x=\pm w_0$ phases, which are a little bit different and cannot be distinguished by eye.

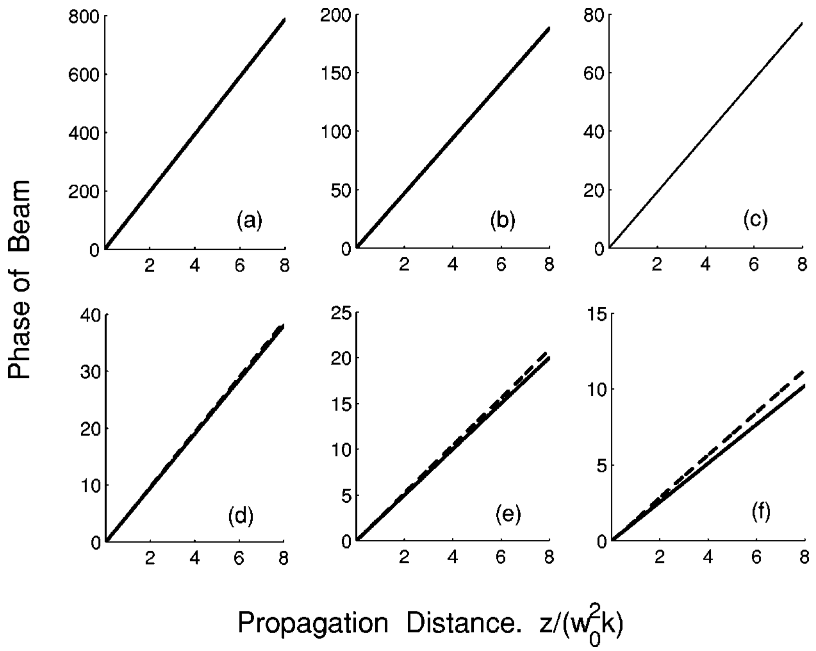

FIG. 8. Comparison of the results about the phase from our model (solid curves) and the numerical simulation (dashed curves) for the $(1+2)$-dimensional beam propagation in the Gaussian-shaped response material when $P_0 = P_c$. Another initial condition is (a) $w_0/w_m = 0.1$, (b) $w_0/w_m = 0.2$, (c) $w_0/w_m = 0.3$, (d) $w_0/w_m = 0.4$, (e) $w_0/w_m = 0.5$, and (f) $w_0/w_m = 0.6$. There are three numerical phase curves a little bit different from each other corresponding to the on-axis and two-side at $\pm w_0$, which cannot be distinguished by eye.

weaker than that in Snyder-Mitchell model, and our model confirms the results about the beam width and phase-front curvature for a single beam obtained from Snyder-Mitchell model in more extensive degree of nonlocality.

VI. CONCLUSION

We discuss the evolution of the optical beam in the strongly nonlocal cubic nonlinear media with the arbitrary symmetric and real-valued response functions. A model is presented, and its exact analytical solution is obtained. The stability property of the solution is rigorously obtained. We show the equivalence of the evolution equation for the beam width to Newton's second law for the motion of a particle in classic mechanics, and the optical spatial soliton is equivalent to the rest state of the particle. A phenomenon is predicted that the phase shift of the strongly nonlocal optical spatial soliton should be large to maintain its propagation. Our analytical results are confirmed by the numerical simulation of the NNLSE. The comparison of our model with Snyder-Mitchell (linear) model shows that our model confirms the results about the beam width and phase-front curvature for a single optical beam from Snyder-Mitchell model in more extensive degree of nonlocality.

Note added. Recently we were happy to have read the latest paper (Ref. [18]). In this paper, it was claimed that the nematic liquid crystals are indeed one of the strongly nonlocal nonlinear media, hence the observed optical spatial solitons in the nematic liquid crystals (see Ref. [19]) are the accessible solitons suggested by Snyder and Mitchell. Before this work, it would be considered that the strongly nonlocal nonlinear media had not been discovered (see, for example, Ref. [10]). Representing the second milestone in nonlocal optical spatial soliton investigations (the first one is Snyder and Mitchell's), this work (Ref. [18]) would stimulate more both theoretical and experimental activities towards a thorough understanding of the nonlocal optical spatial solitons. It would be possible, therefore, that the large phase shift of the strongly nonlocal optical spatial solitons would be observed in the nematic liquid crystals.

TABLE III. The exact numerical results, the analytical results, and their relative errors for the normalized on-axis phase slope $\overline{\phi} = \phi L_R$, where $L_R = w_0^2 k$ is the Rayleigh distance.

w_0/w_m	0.1	0.2	0.3	0.4	0.5	0.6
			$D=1$			
ER	99.25	24.26	10.38	5.53	3.29	2.09
AR[a]	99.25	24.25	10.36	5.50	3.25	2.03
RE(%)	0.0	0.0	0.2	0.5	1.2	2.9
			$D=2$			
ER	98.382	23.459	9.653	4.823	2.614	1.416
AR[b]	98.500	23.500	9.611	4.750	2.500	1.278
RE(%)	−0.12	−0.17	0.44	1.51	4.36	9.75

[a] $\overline{\phi} = w_m^2/w_0^2 - 3/4$.
[b] $\overline{\phi} = w_m^2/w_0^2 - 3/2$.

ACKNOWLEDGMENTS

This work was supported by the National Science Council of China under Contract No. NSC 90-E-FA06-1-4, the National Natural Science Foundation of China under Grant No. 10371045, the Natural Science Foundation of Guangdong Province, China, under Grant No. 031516, and the team project of Natural Science Foundation of Guangdong Province, China, under Grant No. 20003061.

[1] A.W. Snyder and D.J. Mitchell, Science **276**, 1538 (1997).

[2] A.W. Snyder and Y. Kivshar, J. Opt. Soc. Am. B **11**, 3025 (1997); A.W. Snyder, IEEE J. Sel. Top. Quantum Electron. **6**, 1408 (2000).

[3] S. Abe and A. Ogura, Phys. Rev. E **57**, 6066 (1998).

[4] D.J. Mitchell and A.W. Snyder, J. Opt. Soc. Am. B **16**, 236 (1999).

[5] E. Granot, S. Sternklar, Y. Isbi, B. Malomed, and A. Lewis, Opt. Commun. **166**, 121 (1999).

[6] W. Krolikowski *et al.*, Phys. Rev. E **64**, 016612 (2001).

[7] W. Krolikowski and O. Bang, Phys. Rev. E **63**, 016610 (2000).

[8] O. Bang *et al.*, Phys. Rev. E **66**, 046619 (2002).

[9] M. Peccianti, K.A. Brzdakiewicz, and G. Assanto, Opt. Lett. **27**, 1460 (2002); M. Peccianti *et al.*, Appl. Phys. Lett. **81**, 3335 (2002).

[10] Y.R. Shen, Science **276**, 1520 (1997).

[11] Mathematically, this process is quivalent to the expansion of $R(\mathbf{x}-\mathbf{x}')$ within the integral with respect to $\mathbf{x}'$ about $\mathbf{x}'=\mathbf{x}$ to the second order, which reads $R(\mathbf{x}-\mathbf{x}')=R_0+(\mathbf{x}-\mathbf{x}')\cdot\boldsymbol{\nabla}_\perp R_0+(1/2)[(\mathbf{x}-\mathbf{x}')\cdot\boldsymbol{\nabla}_\perp]^2R_0+\cdots$. Because $R(\mathbf{x})$ is symmetrical with respect to $\mathbf{x}=0$, we have that $\partial_{x_i}R_0=0(i=1,2)$, $\partial^2_{x_1x_2}R_0=0$, and $\partial^2_{x_1}R_0=\partial^2_{x_2}R_0$, then $R(\mathbf{x}-\mathbf{x}')=R_0+(1/2)R_0''(\mathbf{x}-\mathbf{x}')\cdot(\mathbf{x}-\mathbf{x}')+\cdots$.

[12] For the (1+1)-dimensional case ($D=1$), the power should be understood to be the power per unit length in the direction perpendicular to the slab-waveguide plane.

[13] $\psi(\mathbf{x},z)$ described by Eq. (2) is power conservative, i.e., $\int|\psi|^2d^D\mathbf{x}=\int|\psi_0|^2d\mathbf{x}=P_0$. By subtracting the multiplication of Eq. (2) with ψ^* from its conjugation, we have $\partial_z|\psi|^2=-2\mu\mathrm{Im}\boldsymbol{\nabla}_\perp\cdot(\psi^*\boldsymbol{\nabla}_\perp\psi)$, the integration of which over $\mathbb{R}^D$ can prove the fact.

[14] The parameter $dw/dz|_{z=0}$ is determined by whether the input Gaussian beam is with its minimum beam radius (beam waist) or not. If this is case, $dw/dz|_{z=0}=0$, otherwise $dw/dz|_{z=0}\neq 0$. However, there is no substaintial difference in the treatment for two different cases.

[15] J.S. Aitchison *et al.*, Opt. Lett. **15**, 471 (1990).

[16] G. P. Agrawal, *Nonlinear Fiber Optics* 3rd edition (Academic Press, London, 2001), Sec. 7.5.2; *Application of Nonlinear Fiber Optics* (Academic Press, London, 2001); G. I. Stegeman and G. Assanto, in *Integrated Optical Circuits and Components: Design and Applications*, edited by E. J. Murphy (Marcel Dekker, Inc., New York, 1999), pp. 381–418.

[17] The three inequalities are $2ab\leqslant a^2+b^2$, $(a+b)^2\leqslant 2(a^2+b^2)$, and $a\leqslant|a|$.

[18] C. Conti, M. Peccianti, and G. Assanto, Phys. Rev. Lett. **91**, 073901 (2003).

[19] M. Peccianti *et al.*, Appl. Phys. Lett. **77**, 7 (2000); M. Peccianti and G. Assanto, Phys. Rev. E **65**, R035603 (2002).